Can Tho University Journal of Science
website: sj.ctu.edu.vn

MODIFIED CONTROLS FOR DOUBLY FED INDUCTION GENERATOR UNDER UNBALANCED VOLTAGE FOR TORQUE STABILITY CONTROLLER

Nguyen Thanh Hai[1,3], Phan Quoc Dzung[2] and Vo Viet Cuong[1]

[1]*Ho Chi Minh City University of Technology and Education, Vietnam*
[2]*Ho Chi Minh City University of Technology, Vietnam*
[3]*Le Hong Phong High School for the Gifted, Ho Chi Minh City, Vietnam*

ARTICLE INFO

Received date: 25/01/2016
Accepted date: 08/07/2016

KEYWORDS

DFIG, PWM, Hysteresis current controller, SFOC, Fuzzy logic

ABSTRACT

This paper presents both the previously and newly modified Stator Flux Oriented Control (SFOC) with Pulse Width Modulation (PWM) and Hysteresis Current Controller (HCC) structures for Doubly Fed Induction Generator (DFIG) in wind turbines to improve responses of active power, reactive power and generator's torque during the grid voltage unbalance. In the proposed SFOC-based scheme, which emphasizes on improvement of generator's torque performance, PI controllers with Fuzzy logic, Notch filters and the Torque Stability Controller (TSC) are utilized. The other control techniques use single or multiple applications of PI controller with anti-windup, hybrid PI-Fuzzy controller with anti-windup and Notch filter to eliminate the second-order harmonic components. The designed system consists of a wound rotor induction generator and power-electronics converters at both rotor and grid sides. The modifications are applied to the rotor side converter (RSC). Simulations in Matlab/Simulink illustrate the enhanced stability of torque, active and reactive powers delivered by DFIG in both the SFOC-based and HCC-based schemes. Moreover, comparisons in simulation results, obtained separately from all the presented control structures, are provided to evaluate the effectiveness of the newly proposed scheme.

Cited as: Hai, N.T., Dzung, P.Q. and Cuong, V.V., 2016. Modified controls for doubly fed induction generator under unbalanced voltage for torque stability controller. Can Tho University Journal of Science. Special issue: Renewable Energy: 18-28.

1 INTRODUCTION

In recent years, Doubly fed induction generators (DFIGs) have been commonly used in variable-speed wind turbines due to its advantages such as converters with slip rating, ease of implementation, and four-quadrant active and reactive power control. The control and operation of the DFIG have been focused on generator modeling, direct power control, fault ride-through capability, and unbalanced grid voltage (Leonhard, 2001; Ackermann, 2003; Wenske, 2011). In these studies, the majority of current control systems for DFIG systems have been mainly developed based on the traditional vector control scheme using a conventional proportional-integral (PI) controller to regulate the current. However, the grids often experience problems such as unbalanced voltage dips, which causes an increase in winding temperature, pulsation of torque and power, oscillations of stator/rotor currents, and mechanical stress on the gear-box (Yikang *et al.,* 2005; Xu *et al.*, 2007). Technical

limitations for connected wind farms to maximize generator's output include voltage and reactive power control, frequency control, and fault ride-through capabilities (Alegría *et al.*, 2007).

The stator voltage's magnitude is determined by the exchange of reactive power between generator and the grid while the phase difference is controlled by active power (Alegría *et al.*, 2007). Therefore, power balance must be maintained on the grid. A voltage drop proportional to current and radial distance to the substations happens when a fault occurs. Due to the remote location of wind farms, the voltage difference may be well out of the limits and this could result in multiple disconnections on the wind farms (Alegría *et al.*, 2007).

The active power delivered to the grid by generator depends on the input mechanical power provided by the wind turbine. Therefore, a mismatch in power supply and demand on the distribution network could lead to a change in rotational energy stored in the generator. This will cause a decrease in frequency if the power supply is insufficient and an increase in frequency if the power supply is excessive (Alegría *et al.*, 2007). Fault ride-through capabilities are necessary for the wind farms to maintain connection to protect the network securities. During a voltage dip, DFIG will increase the demand of reactive power to a level that could cause further suppression of the grid voltage (Alegría *et al.*, 2007). Wind farm disconnection as a result of this will cause a mismatch of power supply and demand and then results in frequency drop.

In addition to maintaining the connection to distribution network during voltage unbalance, generators need to keep providing sufficient powers with acceptable qualities, a modified SFOC based control method is proposed (Yikang *et al.*, 2005), using four command values of rotor current components so as to achieve independent control of P and Q as well as constant torque, or constant active power, or balance stator current, or no oscillation of rotor current (Jiabing *et al.*, 2009; Pham-Dinh *et al.,* 2012).

This paper will investigate the qualities of active powers, reactive powers, and generator's torques under the unbalanced grid voltage dip during transient and steady states for the traditional and modified SFOC and HCC methods of DFIG. In detail, one newly modified control scheme is proposed in this study, and two other control structures were previously suggested in by the authors. The modifications are single or combined applications of PI controller, hybrid PI-Fuzzy controller, Notch filter and TSC to eliminate the negative sequence components. In which, the PI controllers with anti-windup are always used to replace the classical PI controllers even in the SFOC with PWM or HCC.

2 DOUBLY FED INDUCTION GENERATOR MODELLING

This section discusses the control structure for vector control of grid connected doubly fed induction generator. The control methods in Jiabing and Yikang (2009) are based on SFOC, while the methods in Jiabing *et al*. (2009) and this paper are on SFOC with TSC and PWM/HCC using PI-F.

Dynamic model of DFIG with balanced grid voltage in a generally rotating reference frame dq (Pham-Dinh *et al.,* 2013) are considered in this paper. Furthermore, positively and negatively rotating reference frames, which are denoted as dq^+ and dq^- respectively, are also used to develop control model for DFIG during unbalanced voltage dip. These reference frames are presented in the Figure 1.

In SFOC reference frame, where the d axis is attached the stator flux space vector, the following characteristics are obtained:

$$\psi_{ds} = |\psi_s| = L_m i_{ms} \tag{1.1}$$

$$\psi_{qs} = 0. \tag{1.2}$$

The stator voltage equations and stator current of DFIG in a generally rotating reference frame dq as shown in equations (2)

$$V_{ds} = R_s i_{ds} + \omega_s \psi_{qs} + \frac{d\psi_{ds}}{dt}. \tag{2.1}$$

$$V_{ds} = R_s i_{ds} + \omega_s \psi_{qs} + \frac{d\psi_{qs}}{dt}. \tag{2.2}$$

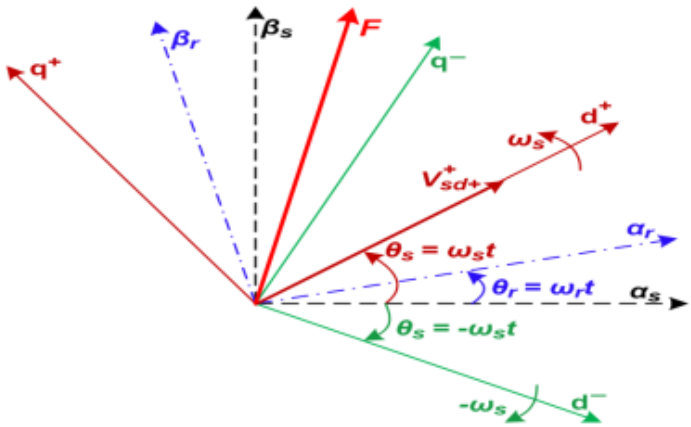

Fig. 1: Relationships between $(\alpha,\beta)_s$, $(\alpha,\beta)_r$, dq^+ and dq^- reference frames

(Pham-Dinh et al., 2013)

2.1 Balanced Network Voltage

If the d-axis of the reference frame is fixed to the stator flux rotating at the synchronous speed of equations in the new reference frame can be derived by simply replacing with in (1), (2) and Figure 1. The equations for active and reactive powers in the stator flux reference frame are shown in equation (3.1) and (3.2).

$$P_s = \frac{3}{2}\left(v_{ds}i_{ds} + v_{qs}i_{qs}\right) = \frac{3}{2}v_{qs}i_{qs} = -\frac{3}{2}|V_s|\frac{L_m}{L_s}i_{qr} \quad (3.1)$$

$$Q_s = \frac{3}{2}\left(v_{qs}i_{ds} - v_{ds}i_{qs}\right) = \frac{3}{2}v_{qs}i_{ds} = \frac{3}{2}|V_s|\frac{L_m}{L_s}\left(\frac{|V_s|}{\omega_s L_m} - i_{dr}\right) \quad (3.2)$$

The equations above have shown that independent control of P and Q can be by controlling i_{dr} and i_{qr} in SFOC.

2.2 Unbalanced Network Voltage

Assuming no zero sequence components, the three phase quantities such as voltage, current, and flux may be decomposed into positive and negative sequence components when the network is unbalanced. In the stationary reference frame, the voltage, current, and flux can be decomposed into positive and negative sequence components as Pham-Dinh *et al.* (2013). According to Figure 1, the transformation between (α, β), $(dq)^+$ and $(dq)^-$ reference frames are given by

$$i^+_{dqr} = i^+_{dqr+} + i^+_{dqr-}. \quad (4.1)$$

$$i^+_{dqr-} = i_{(\alpha\beta)r}e^{-j\varpi_{slip}t} = i^-_{(dq)_{r-}}e^{-j2\varpi_{slip}t}. \quad (4.2)$$

$$i^-_{dqr-} = i_{(\alpha\beta)_r}e^{j\varpi_{slip}t} = i^+_{(dq)_{r-}}e^{j2\varpi_{slip}t}. \quad (4.3)$$

According to (4) and Figure 1 the rotor current is given by

$$i^+_{(dq)_r} = i^+_{(dq)_r+} + i^+_{(dq)_r-} = i^+_{(dq)_r+} + i^-_{(dq)_r-}e^{-j2\varpi_{slip}t}. \quad (5)$$

Substituting (1); (2.1), (2.2), (4.1), (4.2), (4.3) and (5), the equations for active and reactive powers in the stator is as

$$P_s = P_{s0} + P_{s\_\sin 2}\sin(2\omega_s t) + P_{s\_\cos 2}\cos(2\omega_s t). \quad (6.1)$$

$$Q_s = Q_{s0} + Q_{s\_\sin 2}\sin(2\omega_s t) + Q_{s\_\cos 2}\cos(2\omega_s t). \quad (6.2)$$

With

$$\begin{bmatrix} P_{s0} \\ Q_{s0} \\ P_{s\_\sin 2} \\ P_{s\_\cos 2} \\ Q_{s\_\sin 2} \\ Q_{s\_\cos 2} \end{bmatrix} = \frac{3\varpi_s}{2L_s}\begin{bmatrix} 0 & 0 & 0 & 0 \\ -\psi^+_{sd+} & -\psi^+_{sq+} & \psi^-_{sd-} & \psi^-_{sq-} \\ \psi^-_{sd-} & \psi^-_{sq-} & \psi^+_{sd+} & \psi^+_{sq+} \\ -\psi^-_{sq-} & \psi^-_{sd-} & \psi^+_{sq+} & -\psi^+_{sd+} \\ 0 & 0 & 0 & 0 \\ 0 & 0 & 0 & 0 \end{bmatrix}\begin{bmatrix} \psi^+_{sd+} \\ \psi^+_{sq+} \\ \psi^-_{sd-} \\ \psi^+_{sq+} \end{bmatrix} + \frac{3\varpi_s L_m}{2L_s}\begin{bmatrix} -\psi^+_{sq+} & \psi^+_{sd+} & \psi^-_{sq-} & -\psi^-_{sd-} \\ \psi^+_{sd+} & \psi^+_{sq+} & -\psi^-_{sd-} & -\psi^-_{sq-} \\ -\psi^-_{sd-} & -\psi^-_{sq-} & -\psi^+_{sd+} & -\psi^+_{sq+} \\ \psi^-_{sq-} & -\psi^-_{sd-} & -\psi^+_{sq+} & \psi^+_{sd+} \\ \psi^-_{sq-} & -\psi^-_{sd-} & \psi^+_{sd+} & -\psi^+_{sq+} \\ -\psi^-_{sd-} & -\psi^-_{sq-} & \psi^+_{sd+} & \psi^+_{sq+} \end{bmatrix}\begin{bmatrix} I^+_{rd+} \\ I^+_{rq+} \\ I^-_{rd-} \\ I^+_{rq+} \end{bmatrix} \quad (7)$$

The total power imported from the rotor shaft equals to the sum of the power outputs from the equivalent voltage source $j\varpi_s\Psi_s$ and $j(\varpi_s - \varpi_r)\Psi_r$.

$$P_e = -\frac{3}{2}\mathrm{Re}[j\omega_s.\psi_s^+.\hat{I}_s^+ + j(\omega_s-\omega_r).\psi_r^+.\hat{I}_r^+$$
$$= \frac{3}{2}\omega_r.\mathrm{Re}[j\psi_s^+.\hat{I}_r^+] = P_{e0} + P_{e\_\sin 2} + P_{e\_\cos 2} \quad . \quad (8)$$

Where (9)

$$\begin{bmatrix} P_{e0} \\ P_{e\_\sin 2} \\ P_{e\_\cos 2} \end{bmatrix} = \frac{3L_m\varpi_r}{2L_s}.\begin{bmatrix} -\psi_{sq+}^+ & \psi_{sd+}^+ & -\psi_{sq-}^- & \psi_{sd-}^- \\ \psi_{sd-}^- & \psi_{sq-}^- & -\psi_{sd+}^+ & -\psi_{sq+}^+ \\ -\psi_{sq-}^- & \psi_{sd-}^- & -\psi_{sq+}^+ & \psi_{sd+}^+ \end{bmatrix}.\begin{bmatrix} I_{rd+}^+ \\ I_{rq+}^+ \\ I_{rd-}^- \\ I_{rd-}^- \end{bmatrix}.$$

The electromagnetic torque of the DFIG is calculated as

$$T_e = \frac{P_e}{\omega_r} = \frac{P_{e0} + P_{e\_\sin 2} + P_{e\_\cos 2}}{\omega_r}. \quad (10)$$

3 The Proposed Control Methods

3.1 Previously and Newly Proposed Control Schemes

The structure of our formerly modified control method with SFOC for DFIG is represented (Pham-Dinh *et al.,* 2013). The modified control scheme previously and newly proposed one with SFOC are illustrated by Figure 2 and 3 respectively. Converters on the rotor side of DFIG are controlled to achieve the independent control of active and reactive powers. According to Pham-Dinh *et al.* (2013), the control system, using hybrid PI-Fuzzy controller, has provided better performances of the generated powers. However, this is only verified with the balanced grid voltage. To enhance the stability of the powers during voltage unbalance situation, the inclusion of Notch filter has been suggested and shown in Figure 2 and 3. Notch filters are used to eliminate second-order harmonic components in positive and negative sequences of the stator voltage. For the scheme in Figure 2 and 3, Notch filters are used with the positive sequence of stator voltage and the negative sequence of the rotor current.

In Figure 2 and 3, the control scheme proposed in this study, applies TSC to eliminate the negative sequences of the stator voltage which cause distortions in power responses. Additionally, Notch filter is also used to eliminate the second-order harmonic component in the stator voltage. This suggested control scheme reduces the number of current sensors and Notch filter. The decreased amount of computational tasks is achieved with PI controller with Fuzzy.

3.2 PI-F for The Scheme in Figure 2 and 3

Methods to control DFIG's during voltage unbalance conditions include parallel current control techniques operated in the positive and negative sequence reference frames to control the respective positive and negative sequence control currents I^+_{dqr+}, I^-_{dqr-} in the rotor side converters. The parameters of the PI-F are adjusted by the fuzzy rules to obtain the best output to drive the errors to zero. The output of these controllers are commanded values of dq components of rotor current in the stator flux oriented reference frame. These commanded values of currents are used to regulate the RSC for provision of the rotor phase voltage to DFIG

According to (7), (8) it is clear that during conditions of network voltage unbalance conditions the voltage, current and flux all contain both dc values of the positive sequence components and double frequency ($2\omega_s$) ac values of the negative sequence components in dq^+ reference frame. The dc of component regulated normally by the PI controller. However, this controller cannot regulate the double frequency components. The negative sequence control currents I_{dqr-}^- have frequency of $2\omega_s$ (100 Hz) and to control these currents adequately it is thus necessary to use a controller that is tuned to 100 Hz. PI-F rotor side current controller can be implemented for directly controlling both the positive and negative sequence component. The voltage reference output of the PI-F controller can be described as:

$$V_{dqr}^+ = (I_{dqr}^{+*} - I_{dqr}^+)\left\{k_p + \frac{k_i}{s}\right\}. \quad (11)$$

In the scheme described by ω_s is the resonance frequency of the controller. K_p and K_i are the proportional gain and the integral gains respectively. This controller has a very high gain around the resonance frequency and it eliminates the steady state error between the reference and the measured signal. The width of the frequency band around the resonance point depends on the integral gain value. A small value produces a very narrow band, whereas a large value produces a wider band.

3.3 Hysteresis Current Control for The Scheme in Figure 3

The block diagram of the rotor side converter control is shown in Figure 3. The active and reactive powers are compared to their references, and then two PI controllers are used. The outputs of the PI-F represent the direct and quadrature components of the current references. The rotor currents of the DFIG are compared to their references after being sensed and transformed to dq reference frame. The two DC capacitors, which supply the three-level VSI, are assumed with great value in order to neglect the DC capacitor unbalance (Xu *et al.,* 2007). The three phase three-level VSI has three switching commutation cells; each one contains four IGBT and two neutral clamping diodes (see Figure 5).

3.4 Modifications In The Proposed Scheme

The proposed scheme also includes a TSC to obtain less oscillations for torque, active and reactive powers was presented in Hai *et al.* (2015). The commanded values of i^{+}_{dr-}, i^{+}_{qr-} also depended on commanded values of i^{+}_{dr+}, i^{+}_{qr+} which rely on commanded values of P and Q. The Notch filters are assigned to remove the negative sequence components which cause oscillation in active power, reactive power, and electromagnetic torque according to equations (6), (9) and (10) (Hu *et al.,* 2009a).

The proposed scheme is different to the methods in Yikang *et al.* (2005) and Jiabing *et al.* (2009). However, reference values of i^{+}_{dr+}, i^{+}_{qr+} are the output of two PI controllers with fuzzy, as shown in Figure 3, instead of being calculated from equation (5) as in Hai (2014). The PI-F will provide the independence with parameter variations for the commanded values of. Robust responses of the variation of can also be obtained by PI controllers with fuzzy.

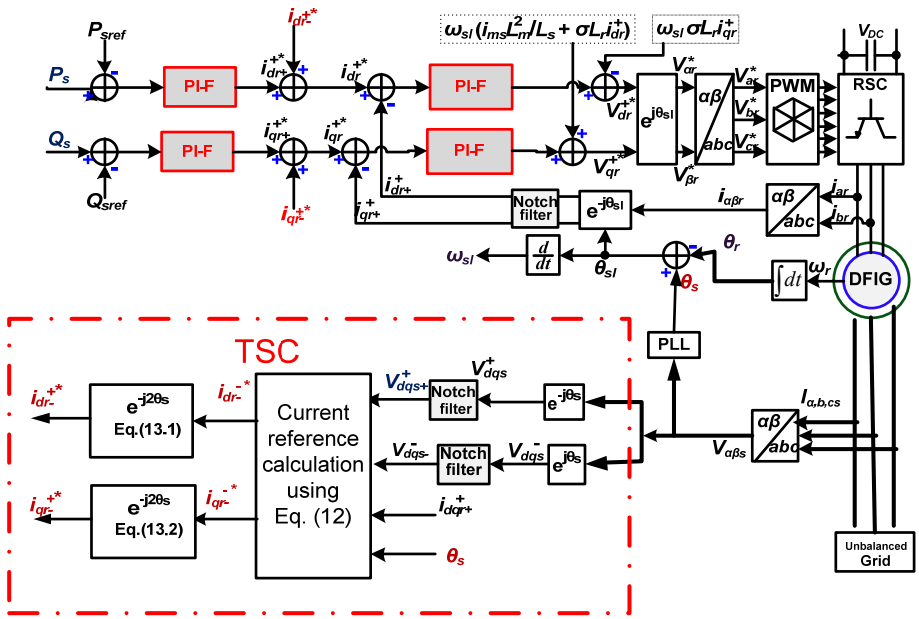

Fig. 2: Proposed control structure with PWM, TSC and PI-F

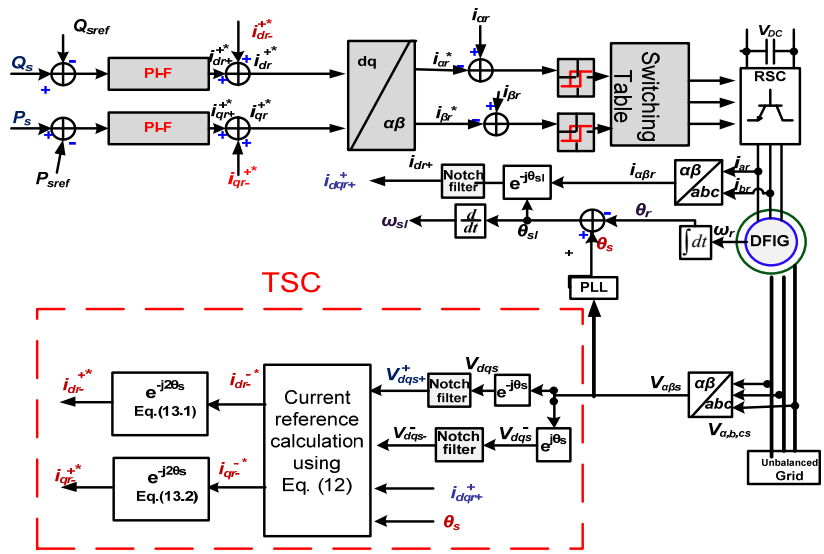

Fig. 3: Proposed control structure with HCC, TSC and PI-F

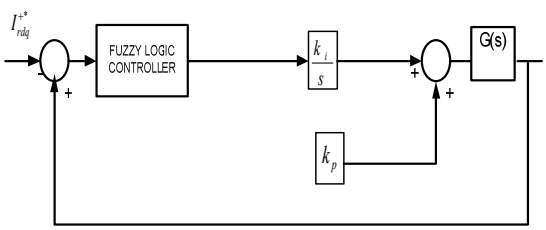

Figure 4: PI-F Controller

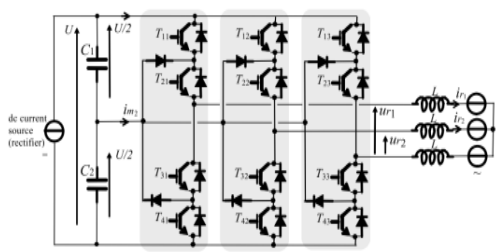

Fig. 5: Three-phase three-level VSI

(Ghennam et al., 2007)

The proposed control schemes in this paper are based on SFOC which is referenced from (Srinadh, 2014). However, reference values of i^{+}_{dqr+} are the output of two PI controllers with fuzzy, as shown in Figure 4, instead of being calculated from equation (12) as in Hai., 2014. The newly proposed scheme is different to the methods in Hai and Cuong (2015). The PI+F controllers will provide the independence with parameter variations for the commanded values of i^{+}_{dqr+}. Robust responses of i^{+}_{dqr+} to the variation of P^*, Q^* can also be obtained with PI controllers with fuzzy. The oscillating terms of the electromagnetic power shown in (7) have to be zero, i.e., $P_{e\_sin2}= 0$ and $P_{e\_cos2}= 0$. Also note that from (9), under such condition, both $Q_{e\_sin2} =0$ and $Q_{e\_cos2}= 0$. With SFOC $\psi^{+}_{sq} = 0$. The commanded values of i^{-}_{dqr-} to achieve constant electromagnetic torque to reduce mechanical stresses on wind turbine are calculated as in equation (11). The calculation is based on the feedback values of the rotor current's positive sequence components in positively rotating reference frame to increase the reliability of the commanded values. Only stator voltages and rotor currents are required.

$$i^{-*}_{dr} = \frac{v^{-}_{ds-}}{v^{+}_{ds+}} i^{+*}_{dr+} + \frac{v^{-}_{qs-}}{v^{+}_{ds+}} i^{+*}_{qr+}. \qquad (12.1)$$

$$i^{-*}_{qr} = \frac{v^{-}_{ds-}}{v^{+}_{ds+}} i^{+*}_{dr+} - \frac{v^{-}_{qs-}}{v^{+}_{ds+}} i^{+*}_{qr+}. \qquad (12.2)$$

The values of i^{+*}_{dr-}, i^{+*}_{qr-} and then i^{+*}_{dr}, i^{+*}_{qr} as in Figure 4 can be done by using equations (13)

$$i^{+}_{(d)_r} = i^{+}_{(d)_{r+}} + i^{+}_{(d)_{r-}} = i^{+}_{(d)_{r+}} + i^{-}_{(d)_{r-}} e^{-j2\varpi_{slip}t}. \qquad (13.1)$$

$$i^{+}_{(q)_r} = i^{+}_{(q)_{r+}} + i^{+}_{(q)_{r-}} = i^{+}_{(q)_{r+}} + i^{-}_{(q)_{r-}} e^{-j2\varpi_{slip}t}. \qquad (13.2)$$

The proposed scheme also includes a TSC which help to Torque Stability, eliminate the negative sequence components of the fundamental frequency and all the harmonics components of stator voltage. The Notch filters are assigned to remove the

negative sequence components which cause oscillation in active power, reactive power, and electromagnetic torque according to equations (6), (7), (8) and (9).

4 SIMULATION RESULTS

Simulations of the proposed control methods for the 2.3MW grid-connected DFIG are carried out with the generator's parameters as given by Table 1. The commanded values of P and Q are changed after 50th second reference value of P is changed from 1.5 MW to 2.0 MW while the reference value of Q is changed from 1.2 MVAR to 800 KVAR. The grid voltages are balanced until the 40th second, one of the phase voltages is reduced by 15%, then they are balanced again from the 80th second. The proposed control methods are for variable speed and constant frequency of DFIG, without loss of generality, the rotor speed in the simulation is super-synchronous and at a particular value of 1400 rpm. The wind speed's variation is shown in Figure 7.

The mean, maximum, and minimum values of the active power, reactive power and machine's torque during the unbalanced voltage from the 55th second to the 65th second are represented in Tables 2 and 3. In detail, the statistics of operations at the sub-synchronous speed n_r= 1400 rpm are also illustrated by these tables.

During the unbalanced voltage, best performances of active power are observed for PWM, then with HCC. In detail, the lowest value of P_{Max} for HCC is -0.5% of the commanded value. In the Figure 9 to 11, the highest value of P_{Min} for the HCC is 0.5% of the set value. Similarly, best performances of reactive power are observed for PWM, then with HCC. In detail, the lowest value of Q_{Max} for the HCC is -0.5% of the commanded value. The highest value of Q_{Min} for the HCC is 1.23% of the set value, Figure 9 to 11.

The simulation results with two different control structures, including the proposed scheme, are shown in Figure 9 to 11 for the active and reactive output powers. These figures demonstrate the power responses when the voltage unbalanced happens (from the time t = 40s) and when the commanded values of powers change (at the time t = 50s) under the voltage unbalance. Besides, Figure 9 to 11 illustrates the torque response of the generator.

Table 1: Parameters of the 2.3MW DFIG

Parameter	Symbol	Value
Stator inductance	L_S	159.2 (μH)
Rotor inductance	L_r	159.2 (μH)
Magnetic inductance	L_m	5.096 (mH)
Stator resistance	R_S	4 (mΩ)
Rotor resistance	R_r	4 (mΩ)
Number of pole pairs	P	2
Frequency (angular)	ω_S	100π (rad/s)
Inertia	J	93.22 (kg.m^2)
Inertia of Rotor	J_{rot}	4.17×10^6 (kg.m^2)

Table 2: Average values of active power (P_s) in the steady state for two controllers

Active Power (P_{sref} = -2MW)	With PWM & PI-F			With HCC & PI-F		
	Min	Mean	Max	Min	Mean	Max
Unbalanced	-2.08	-2.02	-1.95	-2.01	-2	-1.99
(55th - 65th)	3.84%	0.99%	-2.56%	0.5%	0%	-0.5%

$$Deviation = \frac{P_S - P_{Sref}}{P_{Sref}}(\%)$$

Table 3: Average values of reactive power (Q_s) in the steady state for two controllers

Reactive Power (Q_{sref} = 0.8MVar)	With PWM & PI-F			With HCC & PI-F		
	Min	Mean	Max	Min	Mean	Max
Unbalanced	-0.82	-0.805	-0.79	-0.81	-0.8	-0.796
(55th - 65th)	2.44%	0.62%	-1.27%	1.23%	0%	-0.5%

$$Deviation = \frac{Q_S - Q_{Sref}}{Q_{Sref}}(\%)$$

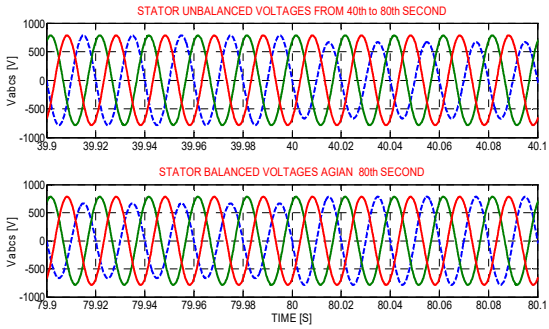

Fig. 6: The grid voltages are unbalanced from the 40th to 80th second

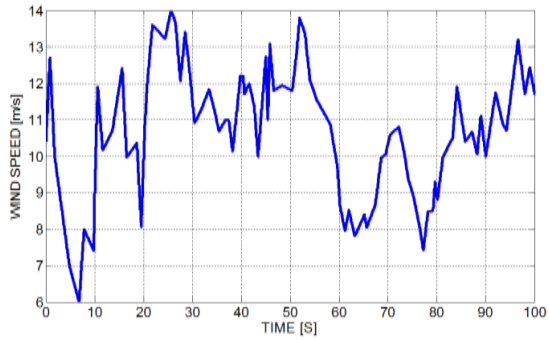

Fig. 7: Random variation of the wind speed

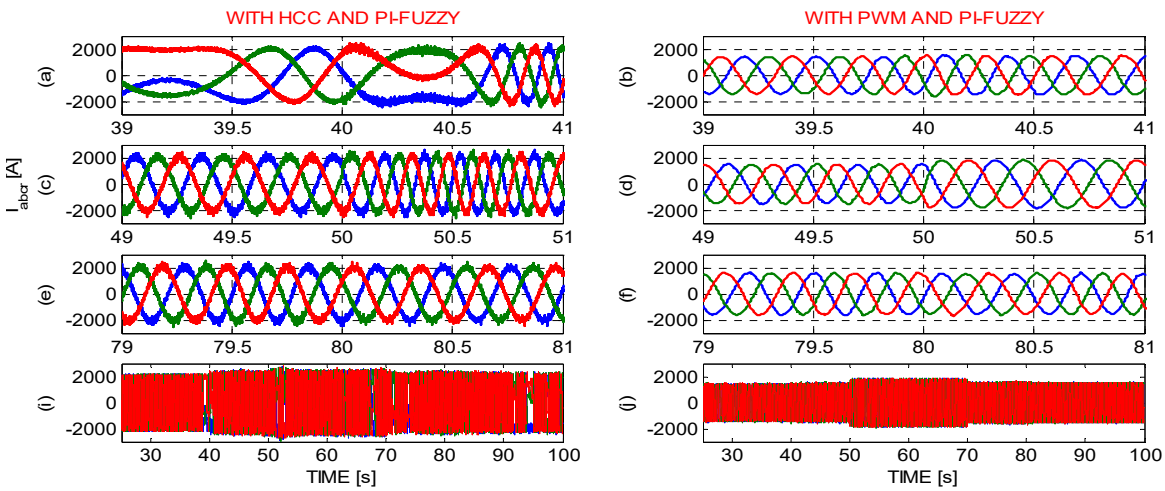

Fig. 8: Rotor current of DFIG (i, j); Rotor current during transient state (a, b)

(c, d) Rotor current of DFIG during unbalanced voltage (unbalanced again from the 40th s)

(e, f) Rotor current of DFIG during unbalanced voltage (balanced again from the 80th s)

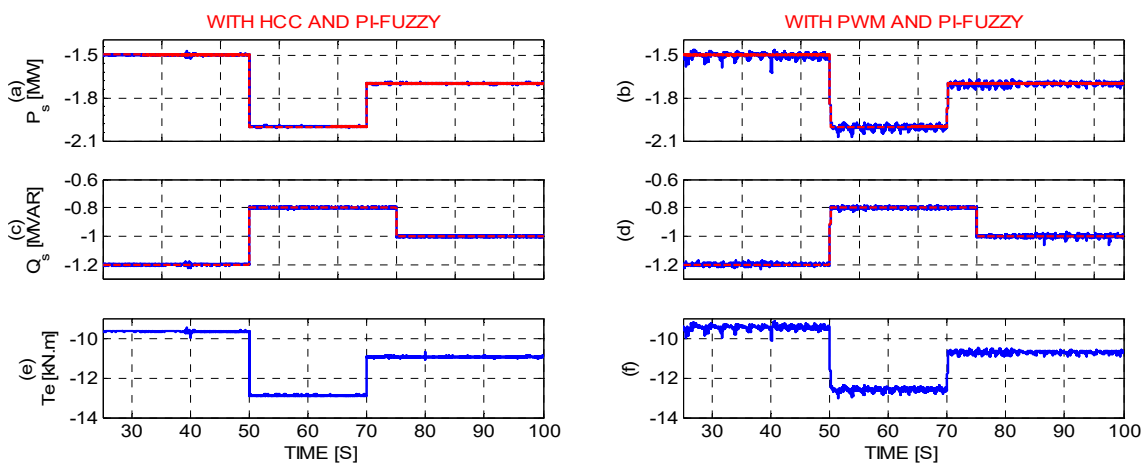

Fig. 9: Active (a, b), reactive (c, d) and torque (e, f) output power of DFIG

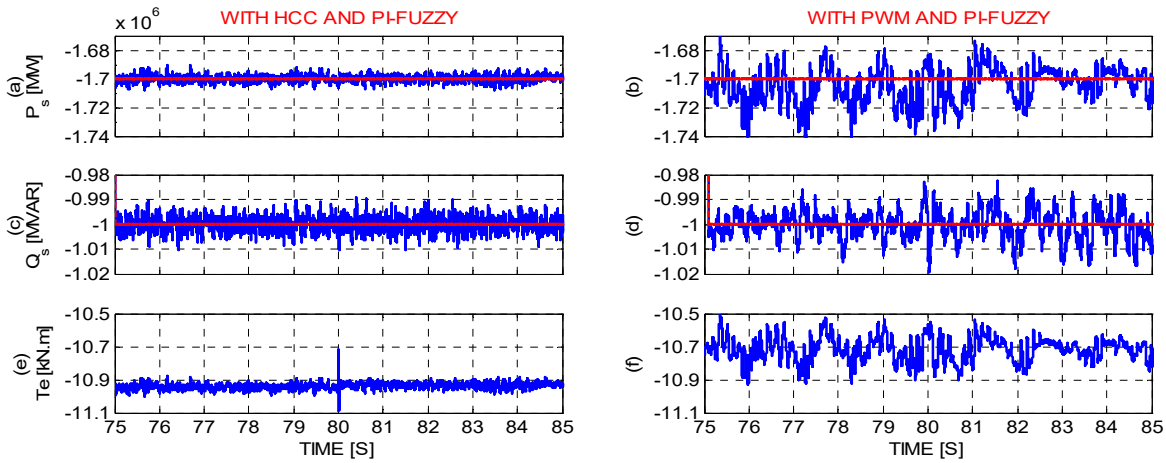

Fig. 10: Active (a, b), reactive (c, d) and torque (e, f) power during unbalanced voltage (balanced again from the 80th second)

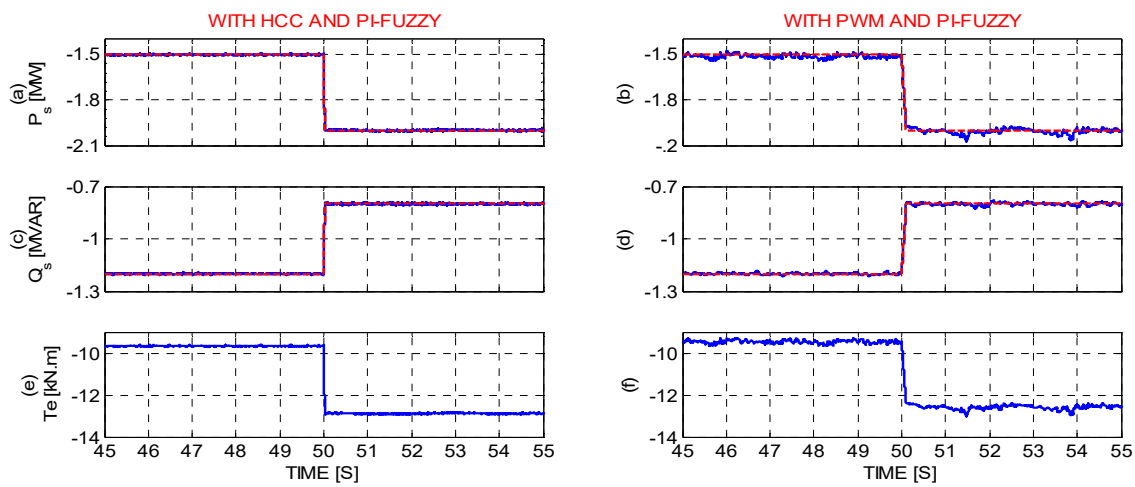

Fig. 11: Active (a, b), reactive (c, d) and torque (e, f) power during transient state

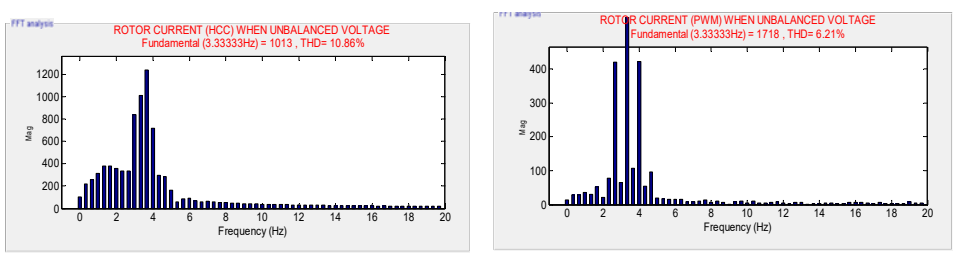

Fig. 12: THD's rotor current when unbalance voltage

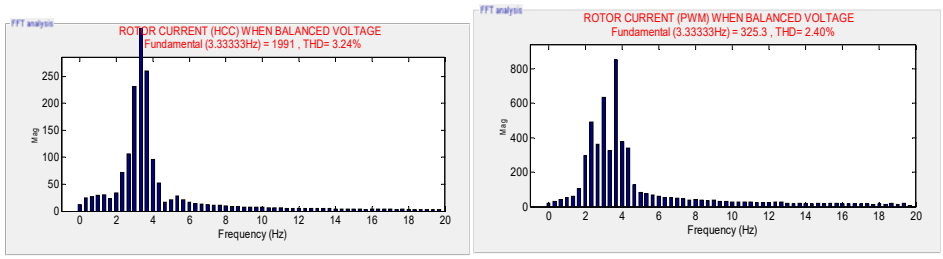

Fig. 13: THD's rotor current when balance voltage

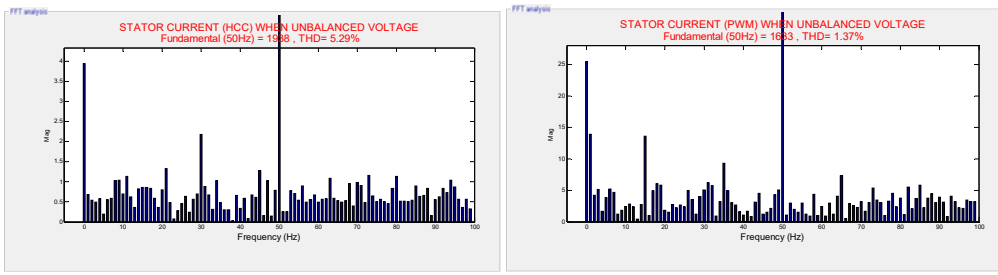

Fig. 14: THD's stator current when balance voltage

5 DISCUSSION

As shown in Table 2, the TSC using PI-F (HCC) methods have shown good steady-state active power responses during the voltage unbalance. In detail, the deviation of the mean value of active power from the reference value is almost zero percent; and the deviation of the maximum and minimum values from the mean value are within 1%. In addition, TSC using PI-F (PWM) is also giving the good performance with small deviation of mean values from reference values about 3.84%. The PWM schemes is active power response when the voltage unbalance happens has higher ripples, while the responses obtained with the two TSC using PI-F for HCC schemes.

As seen in Table 3, steady-state responses of the reactive power are also very good with TSC using PI-F (HCC). In detail, the deviations are ±1.5%. Besides, the deviations of reactive power's mean values for TSC using PI-F (HCC) are also reasonably small during the voltage unbalance. Additionally, higher ripples are observed in reactive power responses of the PWM when the voltage unbalance occurs as described in Figure 10. The observation is also consistent with statistics in Table 3. Figure 10 shows the dynamic responses of reactive powers during transient states.

The TSC using PI-F (PWM) is rotor current response when the voltage unbalance happens has higher ripple, while the responses obtained with the TSC using PI-F (HCC) schemes (see Figure 8).

Harmonic contents of stator current during balanced voltage are quite good for the newly schemes above as shown in Figure 14 and 15 and Harmonic contents of rotor current in Figure 12 and 13. The Total Harmonic Distortion's (THD) are almost the same in these figures. However, during voltage unbalance, with PWM current control gives the best performance in terms of THD. Table 4 illustrates the comparison of THD in the two methods for unbalanced voltages.

Table 4: THD comparison for stator and rotor current

	THD	PWM	HCC
Balanced	Stator current (f = 50 Hz)	**1.3%**	1.7%
Voltage	Rotor current (f= 10/3 Hz)	**2.4%**	3.2%
Unbalanced	Stator current (f = 50 Hz)	**2.7%**	5.3%
Voltage	Rotor current (f= 10/3 Hz)	**6.2%**	10.9%

Total harmonic distortion of the two new control schemes for stator current has been significantly reduced during the unbalanced voltage (2.7% for PWM and 5.3% for HCC), and THD's rotor current (6.2% for PWM and 10.9% for HCC). All the

THD values of stator current are increased during the unbalance.

6 CONCLUSION

The proposed SFOC-based scheme for DFIG with the inclusion of TSC has elevated the stability of the torque response during the grid voltage unbalance when being compared with other modifications of PWM and HCC for better stabilities during the unbalanced voltage dip. This improvement helps to reduce the electrical stress on converters and the mechanical stress on the gear box. Furthermore, the responses of active and reactive power are ameliorated when being compared with a traditional SFOC, although the oscillations are still quite high.

In this study, the observations are made during the occurrence of the voltage dip in one phase, transient states as well as steady states of the powers and torque under the unbalanced condition. When being compared with responses from HCC, the proposed scheme also gives fast responses of active and reactive powers during transient states under the voltage unbalance. In all the observations, the independent controls of the powers are still maintained for the suggested scheme.

Responses of the active power, reactive power, and torque from all the control schemes are observed at the sub-synchronous speed operation when the active power is consumed on the rotor and delivered on the stator of DFIG.

In the future, the experimental verification of the proposed control scheme should be carried out to validate the results obtained in simulations.

REFERENCES

Ackermann, T., 2003. Wind power in power systems; John Wiley and Sons, USA.

Alegría, M.I., Andreu, J., Martín, L.J., 2007. Connection requirement for wind farms: A survey on technical requirements and regulation. Renewable and Sustainable Energy Review. 11(8): 1858-1872.

Ghennam, T., Berkouk, E.M., Francois, B., 2007. A Vector Hysteresis Current Control Applied on Three-Level Inverter. Application to the Active and Reactive Power Control of Doubly Fed Induction Generator Based Wind Turbine. International Review of Electrical Engineering (I.R.E.E.), 20: 258-267.

Hai, N.T., 2014. Improved Control of DFIG Systems under Unbalanced Voltage Dip for Torque Stability Using PI-Fuzzy Controller. International Journal of Electrical Energy. 2(4): 300-307.5

Hai, N.T., 2015. Modified Controls for DFIG under Unbalanced Voltage for Eliminate Rotor Currents Harmonics Using PI-Fuzzy Controller. International Journal of Electrical Energy. 3(1): 6-12.

Hai, N.T., Cuong, V.V., 2015. Modified Controls for Doubly Fed Induction Generator under Unbalanced Voltage Distortion for Torque Stability and PI-Fuzzy Controller. Proceeding of 7th IEEE International Conference on CIS and RAM 2015, pp 65-70, 15-17 July, 2015, Angkor Wat, Cambodia.

Jiabing, H., Yikang, H., 2015. Modelling and enhance control of DFIG under unbalanced grid voltage conditions. Electric Power Systems Research. 79(2): 272-281.

Jiabing, H., Yikang, H., Lie, X., Williams, W.B., 2015. Improve control of DFIG systems during network unbalance using PI-R current regulators. IEEE Transactions on Industrial Electronics. 56(2): 439-451.

Leonhard, W., 2001. Control of electric drives; Springer-Verlag, 3rd edition, USA.

Pham-Dinh, T., Nguyen-Thanh, H., 2013. Improving stability for independent power control of wind-turbine doubly fed induction generator during grid unbalance with PI-Fuzzy controller. Journal of The Japan Society of Applied Electromagnetics and Mechanies. 21(3): 425-429.

Pham-Dinh, T., Nguyen-Thanh, H., Uchida, K., Nguyen, G.M.T., 2013. Comparison between modifications of SFOC and PDC in control of grid-connected doubly fed induction generator under unbalanced voltage dip. Proceeding of SICE Annual Conference 2013, pp. 2581-2588, Nagoya Japan.

Pham-Dinh, T., Nguyen, A.N., Nguyen-Thanh, H., 2012. Improving stability for independent power control of wind turbine doubly fed induction generator with SFOC and DPC during grid unbalance. Proceeding of The 10th International Power and Energy Conference IPEC 2012, pp. 155-160, Ho Chi Minh City, Vietnam.

Srinadh, J., 2014. Dynamic Performance of DFIG using SMES For WECS. International Journal of Recent Development in Engineering and Technology. ISSN 2347-6435(Online). 3(1) 148 – 151.

Wenske, J., 2011. Special report direct drives and drive-train development trends. Wind Energy Report Germany 2011, Siemens Press Picture.

Xu, L., Wang, Y., 2007. Dynamic modeling and control of DFIG based wind turbines under unbalanced network conditions. IEEE Transactions of Power Systems. 22(1): 314–323.

Yikang, H., Jiabing, H., Rende, Z., 2005. Modelling and control of wind-turbine used DFIG under network fault conditions. Proceeding of the Eight International Conference on Electrical Machines and Systems ICEMS 2005. Vol. 2, pp. 986-991, Nanjing, China.